Chapter 3

3.1 Introduction

Solution-processed high-dielectric constant (k) inorganic gate insulators have received much attention as a key element of low voltage thin film transistors (TFTs) due to their low-cost processing.[55, 153, 154] Additionally, their coherent interface formation with solution-processed oxide semiconductors lead to considerable improvements in TFT performance and make it possible to all solution processed TFT fabrication.[10, 155] In particular, low voltage oxide transistors are great interest because of their broad potential for optoelectronics applications, including light emitting transistors and phototransistors.[55, 156] Additionally, low voltage operation makes it possible for low power consuming portable electronics such as cell phone, electronics tab, laptop, etc. Many efforts have been taken before to develop these devices using various sol-gel derived oxide dielectrics, including ion conducting alumina, zirconium oxide, aluminum oxide, etc.[55, 56, 157-161] Apart from these inorganic dielectrics, different types of polymer ion-gels have been employed for low voltage organic polymer TFT fabrication.[162-165] These ion-gel dielectrics are not only suitable for low voltage TFT fabrication but also allow to fabricate printable and flexible TFT. Although this dielectric is not used for solution-processed metal oxide TFT fabrication, which required high processing temperature during the metal oxide semiconductor deposition. On the other hand, inorganic dielectrics are widely used for this purpose because of their good stability during the high-temperature annealing process. Use of such kind of inorganic dielectric can make it possible to fabricate high-quality dielectric-semiconductor interface which is required for high-performance

TFT fabrication. Among all different types of gate dielectric for metal oxide TFT applications, ion conducting sodium beta alumina and related dielectric show the highest performance.[55-57] This class of dielectric fabrication is possible with low-cost solution processing technique like spin or dip coating followed by an annealing step. However, the sodium beta-alumina (SBA) class of materials requires very high annealing temperature (>800 ^{o}C), limiting the accessibility of the substrate materials.

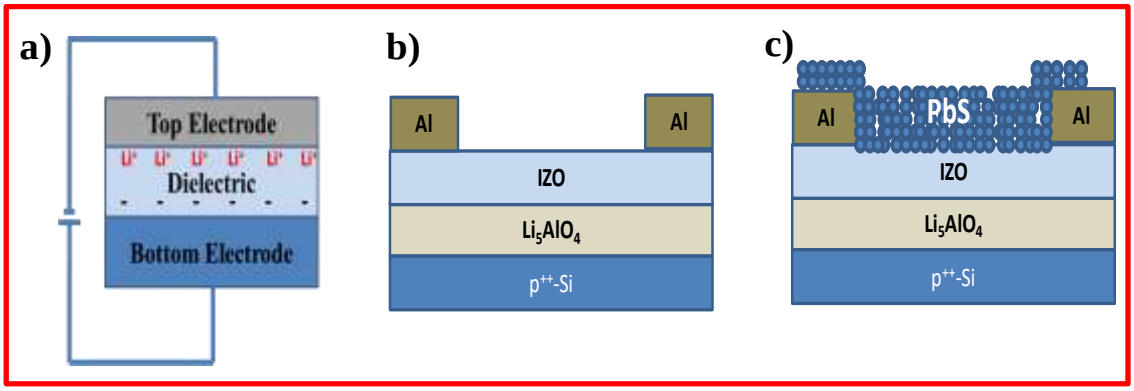

Figure 3.1: *Schematic diagram of* ***a)*** *charge polarization of Li_5AlO_4 dielectric film due to the shifting of Li^+ ion under external bias,* ***b)*** *solution-processed metal oxide IZO TFT and* ***c)*** *IZO/PbS heterojunction phototransistor.*

This crystalline Li_5AlO_4 have two polymorphs recognized by XRD and referred to as α- and β- crystallized phase.[147, 166] Both of this α and β- crystallized phase of Li_5AlO_4 have orthorhombic crystal structure in which aluminum and oxygen (Al & O) are connected in lithium atoms.[147] These crystalline Li_5AlO_4 phases have high ionic conductivity because of loosely bound Li^+ ion that can move easily inside the crystal (**figure 3.1 a)**). In addition, the mobile ion density of this ceramic film is fifty times higher than that of sodium beta-alumina, which is used to fabricate a thin film with higher capacitance. Therefore, the application of such kind of material as a gate dialectic makes the significant improvement of device performance with respect to earlier reported works.

Moreover, it shows much higher performance for low voltage transistor fabricated at significantly lower processing temperature that indicates a great step ahead of the earlier efforts. Solution-processed indium zinc oxide (IZO) transistors have been fabricated using three phases of Li_5AlO_4 dielectric. The detail fabrication of IZO TFT fabrication using Li_5AlO_4 dielectric has been described I chapter-2, paragraph 2.3.1. Among them different TFT, device with α-Li_5AlO_4 shows the best performance. In addition to IZO TFT, IZO/PbS heterojunction phototransistor has been fabricated by overcoating IZO TFT with colloidal PbS quantum dot schematic diagram shown in **figure 3.1 c).** Since the operating voltage of this phototransistor still remains within 2-3 V, the power consumption of this phototransistor is very low with respect to earlier reported metal oxide phototransistor.[167-169]

3.2 Results and discussion

3.2.1 Thermal analysis

The differential thermal analysis (DTA) and thermogravimetric analysis (TGA) of sol-gel derived powder sample were carried out under a nitrogen atmosphere. The combined DTA and TGA results are presented in **Figure 3.2 a).** The DTA data indicates an endothermic event at 277 ^oC, which is associated with the dehydration of the lattice water. Partial removal of structural hydroxyl groups in sol-gel powder also occurs in this region. As a consequence, a weight loss of ~ 8% was observed in TGA data within the temperature range of 270-350 ^oC. However, the major weight loss of about 40% was observed in the range of 356-430 ^oC that corresponds to the decomposition of precursor salts. Most intense exothermic DTA peak was observed at around 450 ^oC, which is associated with crystallization of Li_5AlO_4. A small endothermic peak does also exist at 700 ^oC

corresponding to phase transition of α- Li_5AlO_4 to β- Li_5AlO_4.[170] X-ray diffraction (XRD) study has also confirmed the existence of α- Li_5AlO_4 and β- Li_5AlO_4 phases in the samples annealed at 500 ^oC and 700 ^oC, respectively.

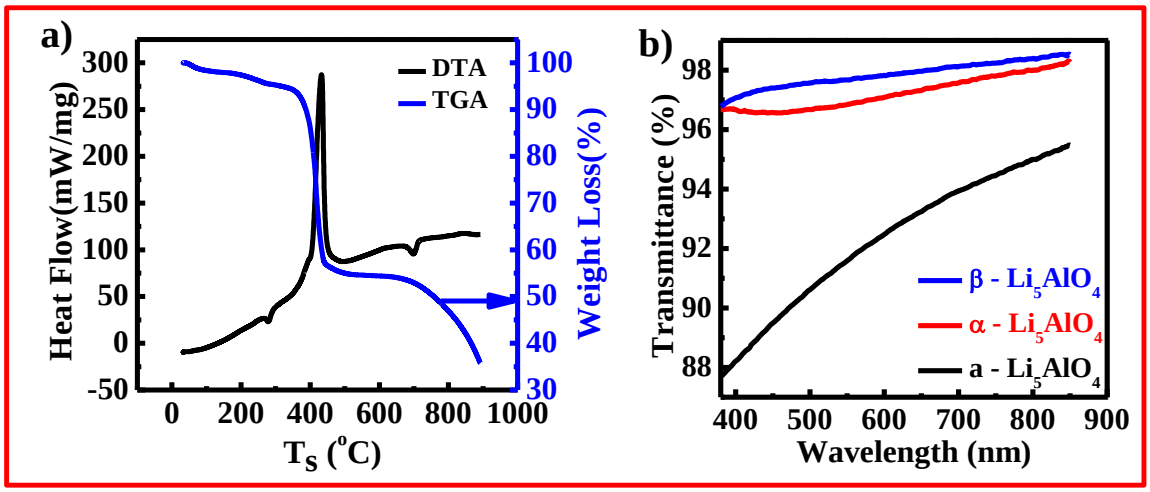

Figure 3.2: a) *Thermal behavior of precursor powder of* Li_5AlO_4 *and* ***b)*** *optical transmittance spectra of* Li_5AlO_4 *thin films annealed at different temperatures.*

3.2.2 Optical properties of Li_5AlO_4 thin films

The optical transmission spectra of Li_5AlO_4 coated glass substrate have been illustrated in **figure 3.2 b**). For this study, clean glass substrates were spin-coated with Li_5AlO_4 precursor solution followed by annealing at 350 ^oC, 500 ^oC and 700 ^oC for 30 minutes under ambient atmospheric condition. As shown in **figure 3.2 b**), all the thin films are highly transparent in the visible region (400-700 nm) with a transmittance over 88%. However, a significant improvement has been observed for the thin film annealed at 500 ^oC and 700 ^oC. This is primarily due to the enhanced scattering from grain defect sites of amorphous Li_5AlO_4 obtained after annealing at 350 ^oC. Film packing and crystalline nature of the thin film are improved at higher temperature annealing and thus scattering

phenomenon gets reduced significantly. Therefore, the sample annealed at 700 ^{o}C exhibits the most transparent film with the transparency of ~ 98%.

3.2.3 Fourier-transform infrared spectroscopy (FTIR)

Fourier-transform infrared spectroscopy (FTIR) measurements were carried out to investigate the existence of precursor salt inside the solution processed Li_5AlO_4 dielectric thin films. **Figure 3.3 a)** shows the FTIR spectra for Li_5AlO_4 dielectric thin film that annealed at 350 ^{o}C, 500 ^{o}C and 700 ^{o}C temperatures respectively. All these thin films have been deposited in the same condition that has been used for TFT fabrication. **Figure 3.3 a)** highlighted the different range of FTIR spectra associated with different precursor groups, including OH^- and COO^-. Between these two groups, the O-H stretching vibration peaks are situated in the range of 3000-3500 cm^{-1} where vibration for COO^- exist at 1430 cm^{-1} and 1500 cm^{-1}.[171-174] However, none of those thin film samples show any peak in these two ranges. Therefore, it is concluded that precursors don't exist in any of these dielectric films.

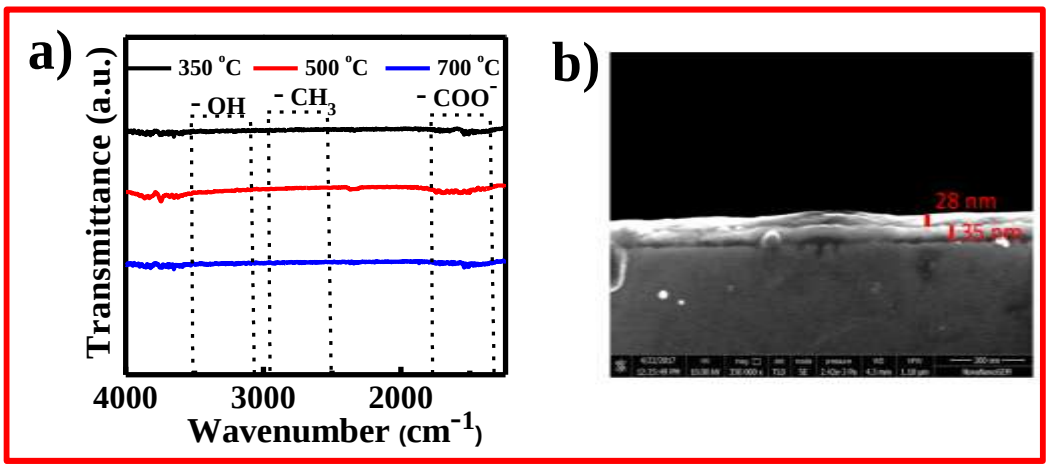

Figure 3.3: ***a)*** *FTIR analysis of Li_5AlO_4 dielectric thin film annealed at 350 ^{o}C, 500 ^{o}C, and 700 ^{o}C,* ***b)*** *cross-sectional scanning electron micrograph of p^{++}-Si/ α-Li_5AlO_4/ IZO film.*

3.2.4 Structural properties of the powder and thin film of Li_5AlO_4

To establish Li_5AlO_4 crystal formation, three different powder gel samples were heated at 350 ^oC, 500 ^oC and 700 ^oC for 30 minutes. A combined XRD data has been shown in **figure 3.4 a).** The data corresponding to the annealing temperature of 350 ^oC shows a feeble peak with broad linewidth revealing the signature of the amorphous phase of Li_5AlO_4. A clear α-Li_5AlO_4 crystal formation has been observed in the sample annealed at 500 ^oC. The diffraction peaks originated from the planes of reflections of (002), (102), (112), (221), (113), (222), (230), (132) and higher indices correspond to those of α-Li_5AlO_4. A distinct β- Li_5AlO_4 phase formation has been observed in the sample annealed at 700 ^oC. Intense peaks are assigned to the reflection planes of (001), (011), (221), (201), (021), (220), (012) and higher indices corresponding to β- Li_5AlO_4 crystal. In addition to the β- Li_5AlO_4 phase, a few additional peaks are observed originated from α-Li_5AlO_4 phase indicating the partial co-existence of α phase in the sample annealed at 700 ^oC.

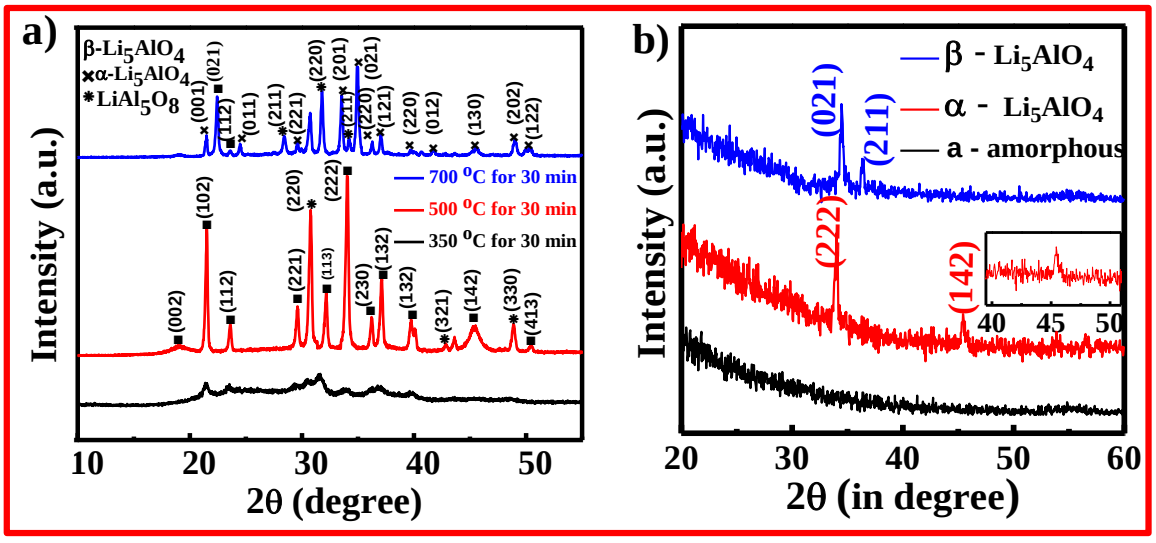

Figure 3.4: a) *XRD pattern of Li_5AlO_4 powder* ***b)*** *Grazing incidence X-ray diffraction (GIXRD) analysis of Li_5AlO_4 dielectric thin film, annealed at 350 ^oC, 500 ^oC and 700 ^oC temperatures in the ambient atmosphere.*

A few additional peaks are also observed in both the samples annealed at 500 ^{o}C and 700 ^{o}C are attributed to the signature of $LiAl_5O_8$ crystal formed as a by-product. Grazing Incidence X-ray Diffraction (GIXRD) analysis was performed with thin film samples formed on a glass substrate, as shown in **figure 3.4 b)**. No peak was observed for an a-Li_5AlO_4 thin film. However, clear (222) and (142) reflections were observed for an α-Li_5AlO_4 thin film sample. In the case of β-Li_5AlO_4 thin film, two closely spaced peaks, (021) and (211), were observed.

3.2.5 Surface morphologies of Li_5AlO_4 thin films

Surface morphologies of p^{++}-Si/Li_5AlO_4 dielectric thin films annealed at different temperatures (350 ^{o}C, 500 ^{o}C and 700 ^{o}C) were investigated by atomic force microscopy (AFM). Representative images for each sample are shown in **figure 3.5**.

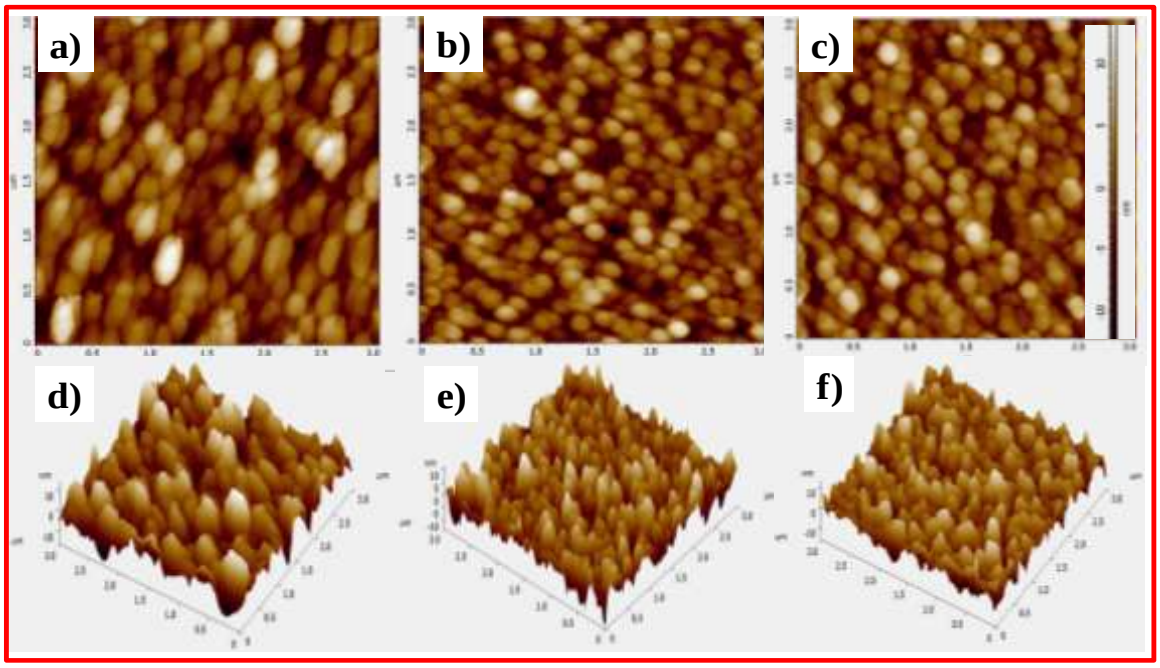

Figure 3.5: *AFM images of Li_5AlO_4 films annealed at **a)** 350 ^{o}C, **b)** 500 ^{o}C, **c)** 700 ^{o}C and 3-D AFM images of same Li_5AlO_4 films annealed at **d)** 350 ^{o}C, **e)** 500 ^{o}C and **f)** 700 ^{o}C from a surface area of 3μm x 3μm.*

The measured root-mean-square (RMS) roughness of the Li_5AlO_4 surfaces annealed at 350 ^oC, 500 ^oC and 700 ^oC are 3.71, 2.84, and 3.12 nm respectively, almost independent of annealing temperature. Additionally, the images show small differences in grain size. However, there are differences in film packing that improves with annealing at higher temperature due to the higher grain density, as shown in **figure 3.5 a) to c)**. This phenomenon can also be realized from 3D AFM images, which are shown in **figure 3.5 d)** to **4f)**.

3.2.6 Capacitance vs frequency measurements

In order to realize the dielectric properties of as-deposited Li_5AlO_4 films, frequency dependence capacitance (C-f) and current-voltage (I–V) measurements have been carried out in a metal–insulator–metal (MIM) device architecture. **Figure 3.6 a)** shows the capacitance of a p^{++}-Si/Li_5AlO_4/Al device with an approximately 35 nm (determined by cross-sectional HR-SEM **figure 3.3b)**) thick Li_5AlO_4 film.

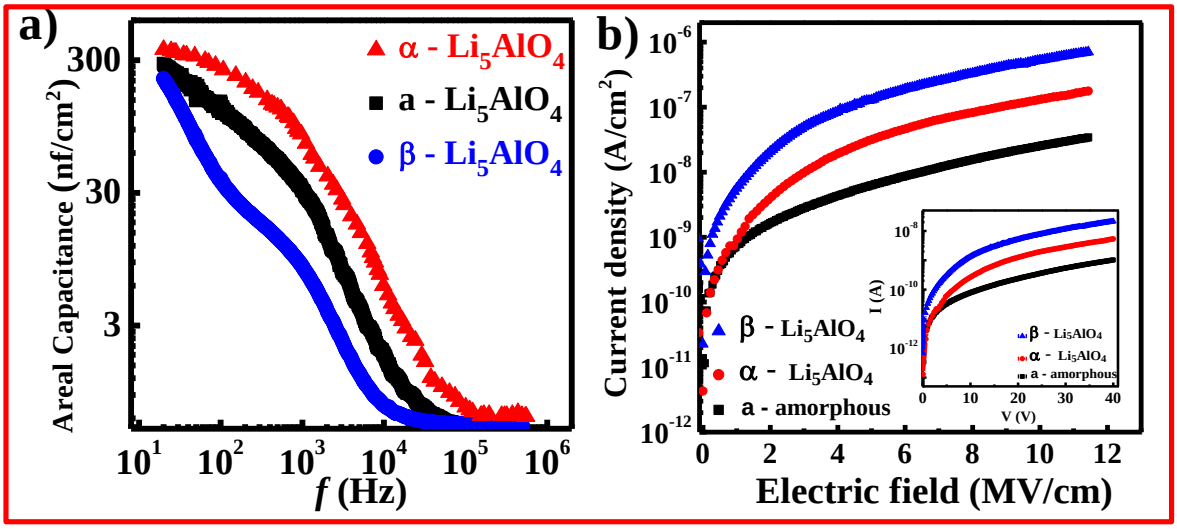

Figure 3.6: a) *Capacitance vs. frequency (C-f) curve and* ***b)*** *leakage current vs. applied electric field curve of Li_5AlO_4 thin film with a device structure of Al/Li_5AlO_4/p^{++}-Si for various types of Li_5AlO_4 dielectric film.*

The capacitance of Li_5AlO_4 film decreases with increasing frequency as expected, which is commensurate with the decrease in polarization response time limited by the ion mobility. The highest capacitance of this film has been obtained with α-Li_5AlO_4 dielectric due to the highest ion mobility of α-phase with respect to other phases of Li_5AlO_4 film. However, the trend of the variation of capacitance for β and a- Li_5AlO_4 are also very similar to α - Li_5AlO_4 dielectric film. Of course, the effective capacitance values of these films are lower than the actual Li_5AlO_4 dielectric film, which is due to the native oxide formation in p^{++}-Si/Li_5AlO_4 interface during the annealing process of dielectric and semiconductor. The effective total capacitance C_{tot} can be obtained from the following equation,[161, 175]

$$\frac{1}{C_{tot}} = \frac{1}{C_{Li_5AlO4}} + \frac{1}{C_{SiO_2}} \text{ .....} \quad \textbf{(3.1)}$$

where $C_{Li5AlO4}$ and C_{SiO2} are the contribution to the total capacitance from Li_5AlO_4 and SiO_2 film respectively. The overall capacitance can be reduced significantly by exploiting the low dielectric constant of SiO_2.

3.2.7 Leakage current density measurements

The current-density and electric field characteristics of the same MIM device are shown in **Figure 3.6 b**). The current density of ~ 2.5 x 10^{-5} A/cm^2 and ~ 2 x 10^{-6} A/cm^2 are observed at 10 and 3 MV/cm operating voltage respectively. The effective source or drain electrode area of our TFT is ~0.06 cm^{-2}. Therefore, the leakage current of our TFT is supposed to be two orders less than the above mentioned current density, which is significantly lower compared to the drain current (I_D). The data implies that Li_5AlO_4 can act as good insulator in our TFT. The I-V characteristic of p^{++}-Si/Li_5AlO_4/Al device also shows that the breakdown voltage of the dielectric film is >40 V **(figure 3.6 b**) inset), which is ~10 times

higher than our typical transistor operation voltage range. Below the breakdown voltage, the I-V characteristic shows reversible behavior. The least current density has been observed for the a-Li_5AlO_4 dielectric device, probably due to the large number of grain boundary that exists in this amorphous phase that interrupts the current conduction path.[10, 173]

3.3 Transistor characterization

Figure 3.7 shows the I_D-V_D and I_D-V_G characteristics of IZO transistors made of Li_5AlO_4 dielectric annealed at different temperatures. All the measurements have been done in the ambient atmosphere. The TFTs were fabricated on p^{++}-Si substrate (as shown in **figure 1.1b**)) with a W/L ratio of 118 (23.6 mm/ 0.2 mm). The applied drain voltage (V_D) was swept from 0 to 2 V for most of the devices and the gate voltage (V_G) were stepped from -0.5 to 2V, depending on the different set of devices. **Figure 3.7 a)** shows the I_D-V_D characteristics of the device with α-Li_5AlO_4 as a gate dielectric annealed at 500 ^oC. The figure indicates the linear and saturation regions of the output characteristics distinctly. Since the breakdown voltage of the α-Li_5AlO_4 is > 40V, a considerable range of applied voltage is accessible to the device under desired operations. **Figure 3.7 b)** shows the I_D-V_G measurement (transfer characteristic) of the same IZO TFT with a source-to-drain voltage (V_D) of 2V.

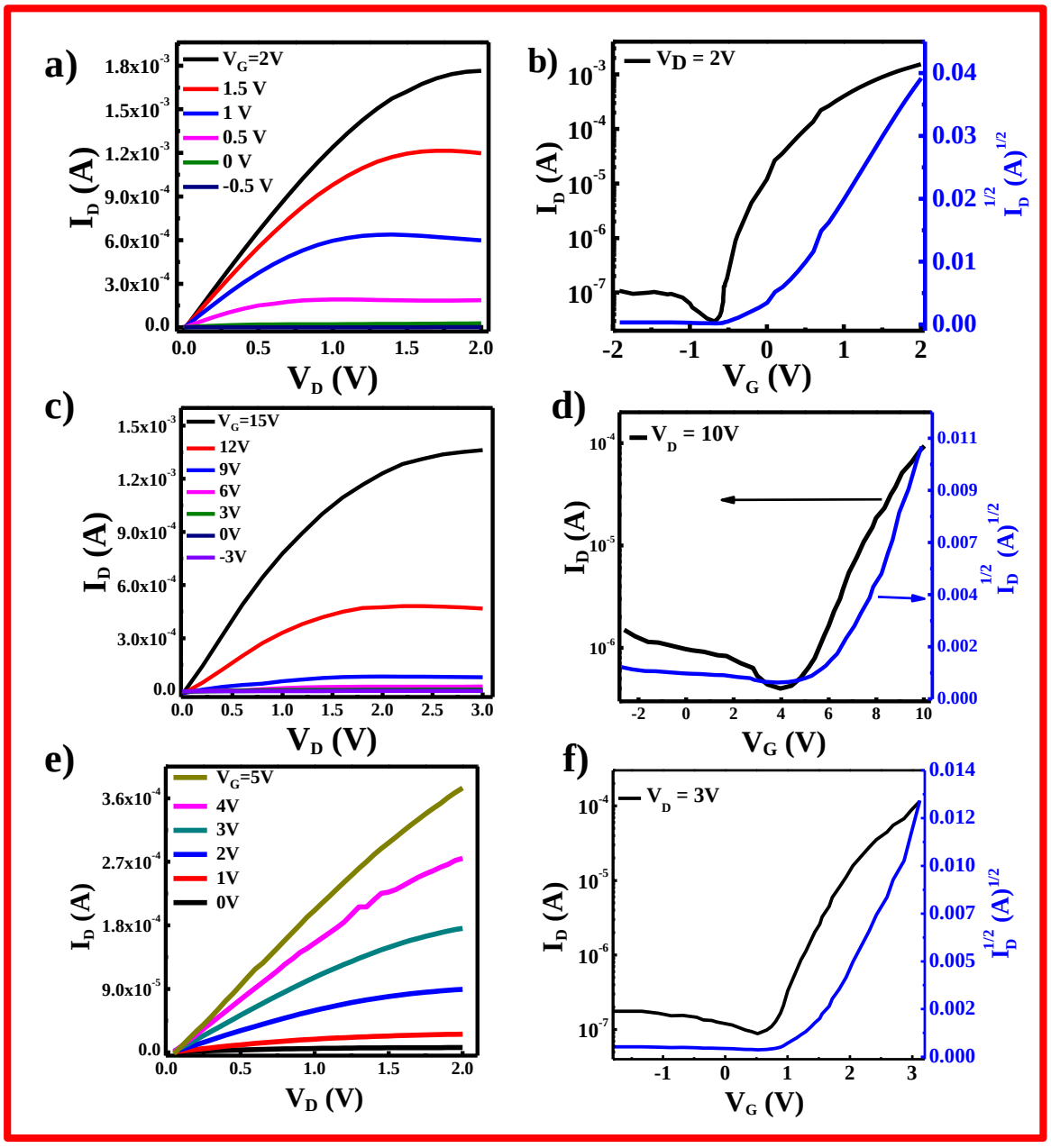

Figure 3.7: *The output characteristics for IZO TFT fabricated with* ***a)*** *α- Li_5AlO_4* ***c)*** *a-Li_5AlO_4* ***e)*** *β-Li_5AlO_4 dielectric. Transfer characteristics for IZO TFT fabricated with* ***b)*** *α-Li_5AlO_4* ***d)*** *a- Li_5AlO_4* ***f)*** *β-Li_5AlO_4 dielectric.*

The gate-source voltage (V_G) was swept between -2V and +2V. The mobility at saturation of this TFT has been calculated from the equation,[10, 176]

$$I_D = \mu C \frac{W}{2L}(V_G - V_{Th})^2 \quad \text{.....(3.2)}$$

To avoid the overestimation of mobility, lower frequency (50 Hz) capacitance has been considered for our mobility calculation.[161] The extracted on/off ratio of the device with α- Li_5AlO_4 dielectric (from **figure 3.7 b))**, is equal to 5 x 10^4 with effective electron mobility of 21.9 $cm^2V^{-1}s^{-1}$, by considering capacitance at 50 Hz-frequency, i.e. 332 $nFcm^{-2}$. It is obvious from equation (3.2) that there is a possibility to achieve significantly high drain current at lower gate voltage provided the product (μC) of mobility and capacitance is a large value. In our case, Li_5AlO_4 film introduces very high capacitance with sufficiently high mobility resulting in a large value of μC. This large value of μC enables our device operating at the lower voltage by achieving high I_D even at low V_G. Around 55 TFT with α-Li_5AlO_4 shows a similar behavior with mobility 21.48 ± 2.16 with threshold voltage ± 0.22 V and subthreshold 0.27 ± 0.16 V (**figure. 3.8**). This data implies the obtained mobility of devices is very similar.

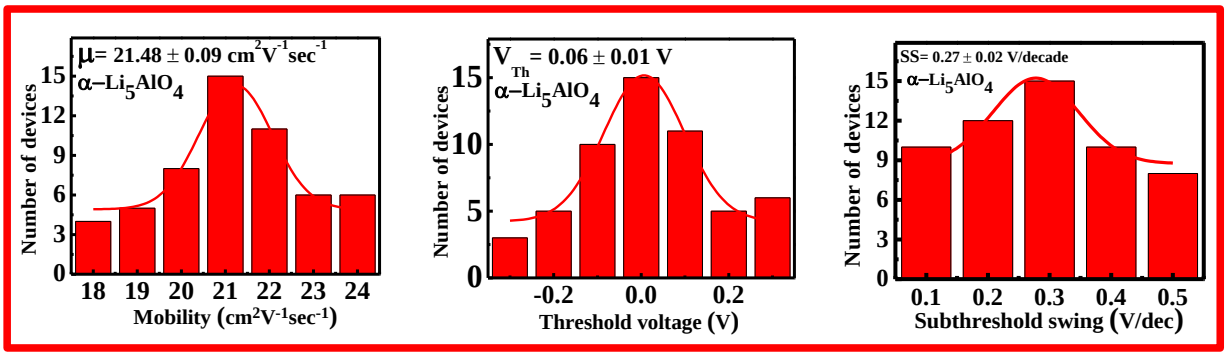

Figure 3.8: *Histograms of the **a)** mobility, **b)** threshold voltage and **c)** subthreshold swing values for Al/IZO/α-Li_5AlO_4/p^{++}-Si TFTs.*

Figure 3.7 e) and **f)** shows the I_D-V_D characteristics of IZO transistors made of β-Li_5AlO_4 dielectric with the same device geometry. In this device, the saturation current requires relatively higher drain voltage compared to that of the α-Li_5AlO_4 dielectric TFT, which is

attributed to the lower capacitance value of β-Li_5AlO_4 dielectric. The electron mobility and the on/off ratio extracted from the I_D-V_G plot shown in **figure 3.7 e) and f)** are 15.5 cm^2 V^{-1} sec^{-1} and 1.31 x 10^3 respectively. Similarly, an IZO FET was also fabricated by using a-Li_5AlO_4 film as gate dielectric **(figure 3.7 c) and d))** and the extracted mobility and on/off ratio are 1.1 cm^2 V^{-1} sec^{-1} and 2.40 x 10^2 respectively.

Among all these three types TFT, α-Li_5AlO_4 dielectric TFT shows the highest mobility, although the difference with β-Li_5AlO_4 dielectric TFT is much higher. Since mobility strongly depends on the semiconductor/dielectric interface, surface roughness plays a crucial role in this difference. Our careful AFM study of three different dielectrics shows that α-Li_5AlO_4 has the least root-mean-square (RMS) roughness. Since β- Li_5AlO_4 has little higher roughness (3.12 nm) which gives effectively lower carrier mobility. The a- Li_5AlO_4 dielectric TFT shows significantly lower mobility mainly because of much lower annealing of IZO (350 ^oC) with respect to the other two different types of TFT. In addition to mobility, α-Li_5AlO_4 dielectric shows the highest Li^+ ion mobility which has been observed in several earlier studies.[148, 150] That higher mobility of Li^+ ion effectively shows the highest capacitance among all three dielectrics. Therefore, the μC value of α- Li_5AlO_4 dielectric becomes significantly higher than the two other types of TFT. The summary of different parameters, including μC and subthreshold swing (SS) of IZO FETs using three different types of Li_5AlO_4 dielectric is presented in **table-3.1**. It is obvious from the comparison that the TFT with α- Li_5AlO_4 film as a gate dielectric reaches the highest μC and least SS value which outperforms the TFT with other gate dielectrics (β-Li_5AlO_4 and a-Li_5AlO_4).

Table 3.1: *The summary of different parameters of IZO TFTs using three different types of Li_5AlO_4 dielectric*

Device no.	**Dielectric**	**W/L**	**C (nF/cm^2) at 50 Hz**	**V_{Th}**	**ON/OFF**	**Electron Mobility (μ) ($cm^2 V^{-1} sec^{-1}$)**	**μC ($nFV^{-1} sec^{-1}$)**
1.	a-Li_5AlO_4	118	150	5.5 V	2.40×10^2	1.1	165
2.	α-Li_5AlO_4	118	332	0.0 V	4×10^4	21.9	7304
3.	β-Li_5AlO_4	118	76	1.25 V	1.31×10^3	15.5	1140

Particularly, the better performance of the TFT with α- Li_5AlO_4 film is attributed to the higher capacitance value of the α- phase Li_5AlO_4 obtained by annealing at 500 ^oC. Overall TFT performance of α-Li_5AlO_4 dielectric thin film has also been compared with recently published other high k-dielectric TFT. From this comparison, it's very clear that the overall μC value of our device is much higher than other reported work.

Although Li_5AlO_4 dielectric contains high concentration Li^+ ion, it doesn't affect TFT stability. To analyze the Li^+ ion effect on TFT stability, two different types of experiments have been done. One of them is the 'bias stress stability' experiment and the other one is the ambient atmosphere storage stability test. For the bias stress stability experiment, transfer characteristic (I_D-V_G sweep) of the α-Li_5AlO_4 dielectric TFT has been performed for 20 minutes with an interval of 30 seconds, which is shown in **figure 3.9 a**). In this presentation, one alternating data has been skip for better presentation. This data clearly shows that there is no variation of I_D-V_G characteristics with different measurements. To test its long term storage stability, we have tested the same transistor for ten days long, which is shown in

figure 3.9 b). This data also shows a very small variation over time as shown in **figure 3.9 c).** Since a very minute amount of ion diffusion to the semiconducting layer can change a significant transport property, therefore it is concluded that no ion diffusion is occurring to the oxide semiconductor. Similar stability experiments have been reported earlier for a number of light ions contain dielectric including H^+, Na^+, Li^+ for metal oxide TFT application and got very similar data like us. [57, 173, 177]

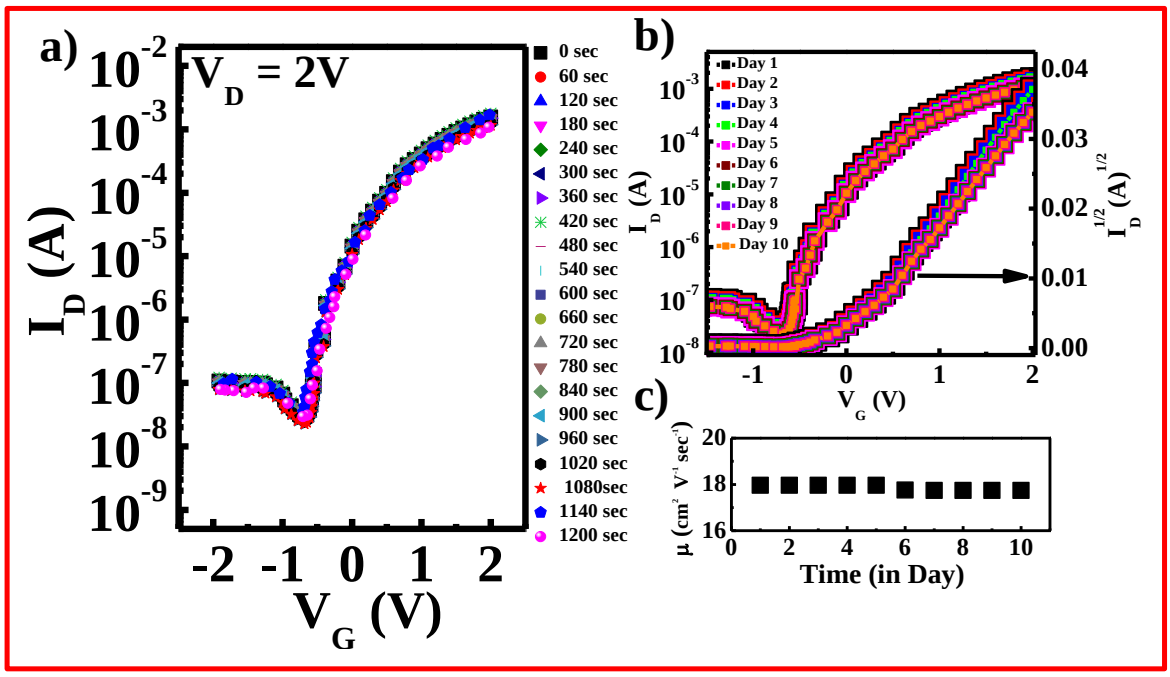

Figure 3.9: *Stability test of the α-Li_5AlO_4 dielectric TFT* ***a)*** *bias stress stability* ***b)*** *ambient atmosphere storage stability* ***c)*** *variation of mobility with time.*

3.4 Phototransistor characterization

The properties of a phototransistor with an IZO/PbS heterojunction were investigated under ambient atmospheric conditions. In a vertical direction to the channel, this heterojunction forms a p–n junction in which PbS QDs act as a p-type semiconductor. Such a kind of

heterojunction is widely studied in PbS-QD based p–n junction solar cells. The reported depletion region of the PbS film of these solar cells is ~200 nm.[178, 179] Since the PbS thickness of these TFT devices is only 25 nm, it is highly expected that the QD layer is fully depleted due to heterojunction formation. The transfer characteristics (I_D–V_G) as shown in **figure 3.10 a)** were measured under white light illumination with various light intensities at V_D = 2 V. In the IZO/PbS heterojunction, PbS has a lower bandgap (1.1 eV), whereas IZO has a relatively wider band gap (3.4 eV). Therefore, under white light illumination, photogenerated excitons (e–h pairs) are mostly generated from PbS QDs. These photogenerated excitons are then separated into electrons and holes due to the barrier potential of the p–n junction that forms in a vertical direction to the channel. During this charge separation process, the electrons transfer to the IZO channel and the holes remain in the PbS layer (as shown in the **figure 3.10 e**)), which effectively reduces the sheet resistance of the channel significantly. Such kind of exciton generation and the subsequent separation rate increase with light intensity. Therefore, the depletion mode current of this heterojunction TFT increases with light intensity. However, the photocurrent generation mechanism of this type of heterojunction photodetector is different from that of a recently published 0D-2D heterojunction photodetector. In those cases, the depletion region is atomically thin and forms a Schottky junction which effectively reduces with additional photogenerated carriers.[180, 181] The responsivity (R) of a phototransistor is determined using the following formula: $R = I_{ph}/PS$, where I_{ph} is the photocurrent ($I_{ph} = I_{light} - I_{dark}$), P is the incident power density and S is the effective illuminated area. The effective irradiated area of this IZO/PbS heterojunction TFT is approximately 11.9 mm^2.

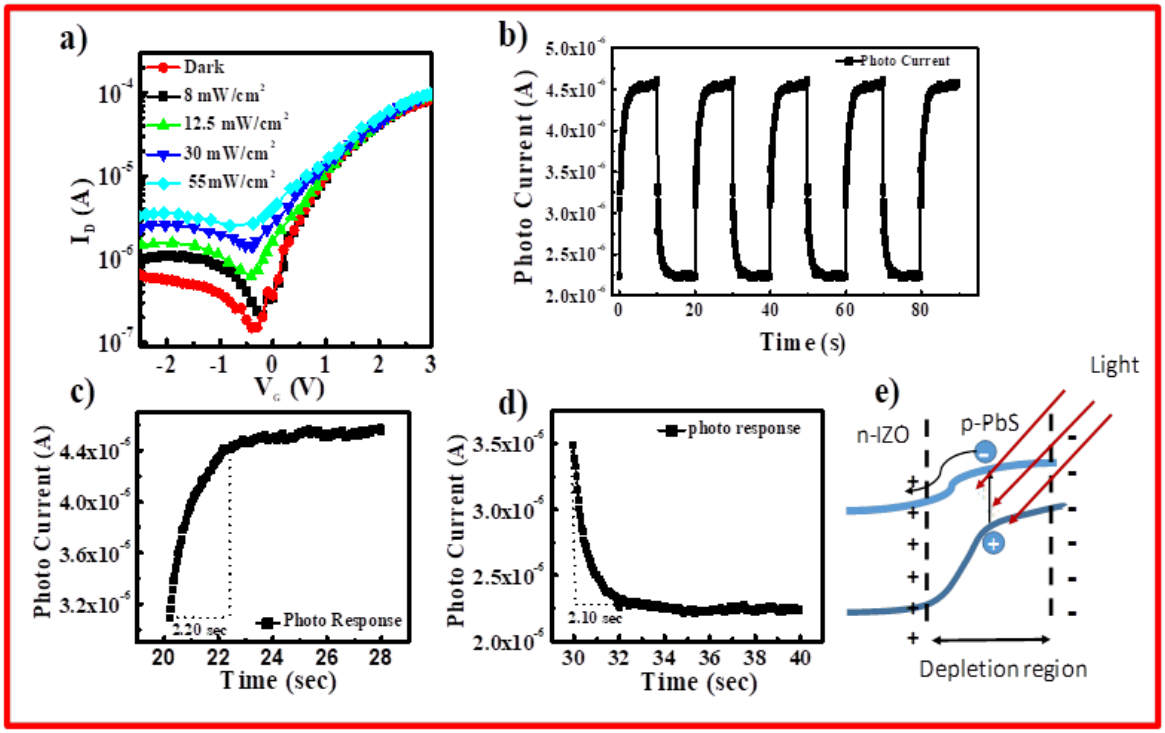

Figure 3.10: a) *I_D-V_G plot of IZO/PbS heterojunction phototransistor under white light illumination* ***b)*** *photo-response data under square shape pulse light illumination* ***c)*** *magnified plot of time response for determination of rise time of device and* ***d)*** *magnified plot of time response for determination of fall time of device* ***e)*** *depletion layer formation of p-PbS/n-IZO heterojunction and photogenerated e-h separation due to the effect of barrier potential.*

The calculated responsivity of this phototransistor is as high as 4.5 x 10^4 AW^{-1} when V_G = -0.4 V and P = 30 mW cm^2 and doesn't change much with different light intensities. To study the photo-response time and the stability of the phototransistors, the device was illuminated with pulsed light **(figure 3.10 b))**. This light signal was generated by biasing a light emitting diode with a square wave of 166 mHz. The rise time of this device is ~2.2 s, whereas the decay time is ~2.1 s as shown in **figure 3.10 c) and d)**, which is comparable to those of previously reported heterojunction phototransistors.[182, 183]

3.5 Conclusions

In summary of this chapter, ion conducting Li_5AlO_4 dielectric thin film was fabricated by the sol-gel technique. These sol-gel derived films were annealed at 350 -700 ^oC to achieve different phases of Li_5AlO_4. It was observed that a-Li_5AlO_4, α- Li_5AlO_4 and β-Li_5AlO_4 could be obtained by annealing the sol-gel-derived film at 350 ^oC, 500 ^oC and 700 ^oC respectively. A solution processed IZO TFTs were fabricated by employing all these three different types of Li_5AlO_4 dielectric which required 2-3 V to operate the devices. Among all the devices, TFT made of α- Li_5AlO_4 dielectric required the least voltage to saturate the drain current in I_D-V_D plot and showed the highest mobility too, suggesting the best candidate for low voltage TFT application. This device showed effective electron mobility of 21.9 $cm^2V^{-1}s^{-1}$ with an On/Off ratio of 5x 10^4. This value is much better than that of the TFT device fabricated with sodium beta-alumina (SBA) dielectric on p^{++}-Si substrate reported previously[55]. These data suggest that the higher concentration of a mobile ion in Li_5AlO_4 film compared to SBA is responsible for this improved performance of the TFT device. In addition, the Li_5AlO_4 film required 500 ^oC processing temperature to attain the crystalline phase of the dielectric which is ~300 ^oC lower than the temperature needed for SBA, indicating the significant improvement of ion conducting dielectric film fabrication for TFT applications. Finally, metal oxide/quantum dot heterojunction phototransistor has been fabricated by coating IZO TFT with colloidal PbS QDs. The responsivity and the response time of the devices are measured as 4.5 X 10^{-4}A/W and 2.2 sec, respectively.